Applied Catalysis B: Environmental 144 (2014) 425–434

Contents lists available at ScienceDirect

Applied Catalysis B: Environmental

journal homepage: www.elsevier.com/locate/apcatb

A novel CoO_x/La-modified-CeO_2 formulation for powdered and washcoated onto cordierite honeycomb catalysts with application in VOCs oxidation

Diana M. Gómez [a], José M. Gatica [a], Juan C. Hernández-Garrido [a], Gustavo A. Cifredo [a], Mario Montes [b], Oihane Sanz [b], José Manuel Rebled [c,d], Hilario Vidal [a,*]

[a] Departamento de Ciencia de Materiales e Ingeniería Metalúrgica y Química Inorgánica, Universidad de Cádiz, 11510 Puerto Real, Spain
[b] Departamento de Química Aplicada, UFI 11/56, Universidad del País Vasco UPV/EHU, Apdo. 1072, 20080 San Sebastian, Spain
[c] LENS-MIND-IN2UB Departament d'Electrònica, Universitat de Barcelona, Barcelona 08028, Spain
[d] Institut de Ciència de Materials de Barcelona-CSIC, Campus UAB 08193, Spain

ARTICLE INFO

Article history:
Received 25 April 2013
Received in revised form 16 July 2013
Accepted 19 July 2013
Available online 29 July 2013

Keywords:
Cobalt catalysts
La-modified-CeO_2
Honeycomb monolith
VOCs oxidation
Washcoating

ABSTRACT

A novel Co (15 wt.%)/La-modified-CeO_2 catalyst was prepared for the oxidation of toluene and ethyl acetate, showing lower light-off temperature (around 20–40 °C) than that of a Pt (3 wt.%)/La-CeO_2 catalyst under the same experimental conditions. Upon washcoating onto cordierite it was still more active than the noble metal reference. The activity remained stable even after 80 h of reaction. Adherence tests indicated a 98% stability of the washcoat, while SEM–EDS study evidenced its homogeneous distribution on the cordierite. ICP analysis and X-ray diffraction demonstrated that the composition and cobalt phase (Co_3O_4) of the powdered catalyst were the same in the washcoat. Moreover textural properties improved according to N_2 physisorption studies due to inclusion of colloidal alumina in the slurry.

1. Introduction

Catalytic combustion of VOCs is one of the most extended techniques used to reduce their emissions due to its high efficiency at a very low pollutants concentration, low energy consumption and low production of secondary pollutants [1]. Several types of catalyst, such as supported noble metals or transition metal oxides are used for VOCs oxidation. The latter have the additional advantage of having lower cost and achieving higher thermal stability and greater resistance to deactivation by poisoning [2]. Within the transition metal oxide catalysts, cobalt containing catalysts present very interesting properties for VOCs oxidation showing high activity for the combustion of ethyl acetate and toluene. Several authors have investigated these reactions using mainly cobalt supported on Al_2O_3 [3], silica [4,5], and zeolites [6]. Good performances in the oxidation of toluene have been also reported by Lamonier et al. [7], who point to the important role played by the redox properties of the catalysts in this reaction. It is well known that the use of some rare earth elements allows increasing the reducibility, ceria being the most notable element employed because its oxygen storage capacity, associated with the Ce^{4+}/Ce^{3+} redox couple, ensuring more oxygen availability for the oxidation process. On the other hand, the incorporation of La^{3+} into ceria enhances its oxygen transfer capability [8,9], its textural stability [10] and its basicity [11]. The latest is an important feature for VOCs combustion since basic oxides tend to favor formation of surface oxygen species, which lead to the complete oxidation of hydrocarbons to CO_2 [12]. Although many researchers have studied VOCs oxidation on ceria-supported cobalt catalysts [12] and Co_3O_4–CeO_2 mixed oxides [13,14] where the Co_3O_4 spinel and CeO_2 fluorite structure were detected, the most frequently reported Co–La–Ce-containing catalysts are Ce-based oxides as supports for $LaCoO_3$ perovskite [15], Ce-substituted $LaCoO_3$ perovskite [16] or perovskite-like materials [17]. There are so far limited results in the literature where the active phase contains Co–La–Ce having a structure different to perovskite-type oxide such as the mesoporous La–Co–Ce–O and La–Ce–Co–Zr–O catalysts, prepared by citric acid complexation and organic template decomposition method by Meng et al. to be evaluated in the CO and propane oxidation [18,19]. The method proposed by these authors produced La–Co–Ce–Zr–O mixed oxides coexisting with a segregated cobalt spinel phase.

The use of structured catalysts as those supported onto honeycomb monoliths has been long considered in the chemical industry

* Corresponding author. Tel.: +34 956 012744; fax: +34 956 016288.
E-mail address: hilario.vidal@uca.es (H. Vidal).

0926-3373/$ – see front matter © 2013 Elsevier B.V. All rights reserved.
http://dx.doi.org/10.1016/j.apcatb.2013.07.045

and it has increased with the significance of environmental catalysis in pollution abatement applications as the catalytic combustion of VOCs [20]. Abatement using such catalysts is suitable when the emission mixtures are complex and total VOC concentration oscillates from low values (ppm order) to rather high concentrations [21], hence catalysts with a high attrition resistance and a low-pressure drop are required. In addition the thin catalytic coating allows high efficiency and selectivity [20,22,23]. The honeycomb monoliths can be made of ceramic or metallic materials. More extensive studies on ceramic monoliths exist due to their wide use in three-way automobile catalysts, mainly cordierite, commonly used, among others, owing to its large-scale production based on extrusion which is quite cheap. Cordierite offers high mechanical strength, high resistance to elevated temperatures and temperature shocks due to its low thermal expansion coefficient. Moreover it presents great adhesion stability, which is a very important property for the monolithic catalysts [22,24]. The most usual way to coat structured supports like honeycomb monoliths, is the well-known washcoating procedure. The monolith is dipped in the slurry prepared with the catalytic material and after a certain time withdrawn carefully. The characteristics of the final coating are a complex function of monolith properties, slurry properties and preparation conditions [22].

In the above context, the purpose of this work has been to prepare a CoO_x/La-CeO_2 catalyst by means of a simple impregnation method to evaluate their performance in the oxidation of toluene and ethyl acetate. Toluene was chosen as a representative VOC of saturated aliphatic hydrocarbons and ethyl acetate of esters, both compounds being widely used in the industry [25]. The powdered catalyst has been deposited by washcoating onto a cordierite honeycomb to compare their behavior in the same reactions; moreover a study of the catalytic stability under reaction conditions was performed. Both, the powdered and the monolithic catalyst have been characterized by means of ICP analysis, N_2 physisorption, X-ray diffraction and scanning electron microscopy (SEM) with EDS analysis. Additionally adherence tests have been used to check the good stability of the washcoat on the cordierite.

To our knowledge no previous studies on Co–La–Ce containing catalysts deposited over honeycomb ceramic monoliths have been reported. Therefore, this new design along with the lack of literature on the application of such catalysts on the combustion of oxygenated VOCs such as ethyl acetate (most existing references are focused on methane, toluene, benzene or propene) should be considered major novelties of the work here presented.

2. Experimental

2.1. Materials

High surface area cerium dioxide was supplied by Rhodia. Highly pure reagents including $La(NO_3)_3{\cdot}6H_2O$ purity 99.9% supplied by Aldrich Chem. Co. and an aqueous dissolution of $[Pt(NH_3)_4]{\cdot}(OH)_2$ with a Pt content of 9.09% purity 99.9% from Alfa Aesar and $Co(CH_3COO)_2{\cdot}4H_2O$ purity 98% provided by Panreac were also used. The monolithic substrates used (Fig. 1) were obtained by cutting a commercial cordierite honeycomb piece from Corning Inc. with a square cell density of 400 cells per square inch (cpsi), wall thickness (t) of 0.21 mm, geometric surface area (GSA) of 27 $cm^2\,cm^{-3}$, open frontal area (OFA) of 65%, hydraulic diameter (D_h) of 0.99 mm and with composition of 19.00% Al, 22.10% Si, 7.80% Mg and 0.37% Fe (wt% estimated by ICP analysis). To obtain stable slurries two additives were used: a commercial colloidal alumina AL20 from NYACOL (20% in weight of Aluminum Hydroxide Oxide) and polyvinyl alcohol (PVOH 4/88, Fluka).

2.2. Catalysts preparation

2.2.1. Preparation of powdered catalysts

The La(6.84 wt%)-modified-CeO_2 material used as catalytic support was prepared by incipient wetness impregnation of ceria using $La(NO_3)_3{\cdot}6H_2O$ as precursor. The lanthanum content was selected in a preliminary study in which this variable ranged from 1.7 to 17.2 wt% searching for the best textural properties. This sample was calcined at 500 °C for 4 h and it was labeled hereafter as La-CeO_2. BET surface area and pore volume (non microporous sample) were 89.2 $m^2\,g^{-1}$ and 0.127 $cm^3\,g^{-1}$, respectively. The CoO_x/La-modified-CeO_2 catalysts with nominal loading of 15 wt% of cobalt (labeled as Co/La-CeO_2) was prepared by impregnating La-CeO_2 with an aqueous solution of $Co(CH_3COO)_2{\cdot}4H_2O$ with excess of solvent (distilled water). After its removal by rotary evaporation at 60 °C, the sample was dried at 120 °C for 4 h followed by calcination in a muffle furnace in air at 450 °C for 2 h. For the sake of comparison, 3 wt% Pt/La-modified CeO_2 catalyst, named (Pt/La-CeO_2) was also prepared by incipient wetness impregnation method using the same ceria based oxide as support and $[Pt(NH_3)]_4{\cdot}(OH)_2$ in aqueous dissolution as Pt precursor. In addition, a CoO_x/CeO_2 catalyst with nominal loading of 20 wt% of cobalt (labeled as Co/CeO_2) was prepared following the same procedure of Co/La-CeO_2 applied to a lanthanum-free ceria support to evaluate the influence of this promoter.

2.2.2. Optimization of the slurry and preparation of the monolithic catalysts

The particle size distribution of the powdered sample was monitored by laser diffraction with a MasterSizer 2000 of Malvern Instrument Ltd. For these measurements, 100 mg of solid were dispersed in 20 ml H_2O and the pH was adjusted to 4.0 with acetic acid. Three measurements were recorded to check the reproducibility. In all cases the observed values presented a negligible standard deviation. The d_{90} value was calculated by the Malvern Instrument software. This value corresponds to the diameter below of which 90% of the population lies.

The zeta potential was measured by using a MALVERN Zetasizer 2000 Instrument. The powdered catalyst was dispersed in 50 ml of a 1.0 mM NaCl solution. Zeta potential curves as a function of pH were obtained by preparing six samples with different pH adjusted with acetic acid or ammonium hydroxide.

The viscosity of the slurries was measured using a AR 1500ex rheometer from TA Instruments with a rotor HA AL Recessed (diameter: 28 mm, length 42 mm) at 25 °C. Approximately 7 ml of sample were used for the experiment. The sample was exposed to an increasing shear rate of 3–3715 s^{-1} and the viscosity value was taken at 3400 s^{-1}.

The cordierite honeycomb block was cut with a hollow drill with diamond cutting edge to obtain cylindrical pieces with a diameter of 16 mm, a length of 30 mm and a weight of approx. 2.6 g. Polyvinyl alcohol (0.09 $g\,g_{cat}^{-1}$) and colloidal alumina (0.22 $g_{Al_2O_3}\ g_{cat}^{-1}$) were used as additives for obtaining stable aqueous slurries and as binder respectively. The pH of the slurries was adjusted by using acetic acid. The cordierite monoliths were dipped into the slurry at 3 cm min^{-1} and maintained immersed for 1 min. They were withdrawn at the same speed and the slurry excess of the slurry was eliminated by centrifugation at 400 rpm for 2 min followed by air blowing. The coated samples were dried at 120 °C for 30 min and weighted to estimate the weight gain. This washcoating procedure was repeated as many times as required to obtain the desired amount of coating and finally the monoliths were calcined at 450 °C for 2 h. Thus, Co/La-CeO_2/cordierite monolithic catalysts with three different catalyst loadings (around 125, 250 and 500 mg per monolith, labeled as MC125, MC250 and MC500 Co/La-CeO_2 respectively) were obtained. The remaining slurry was dried and calcined at the

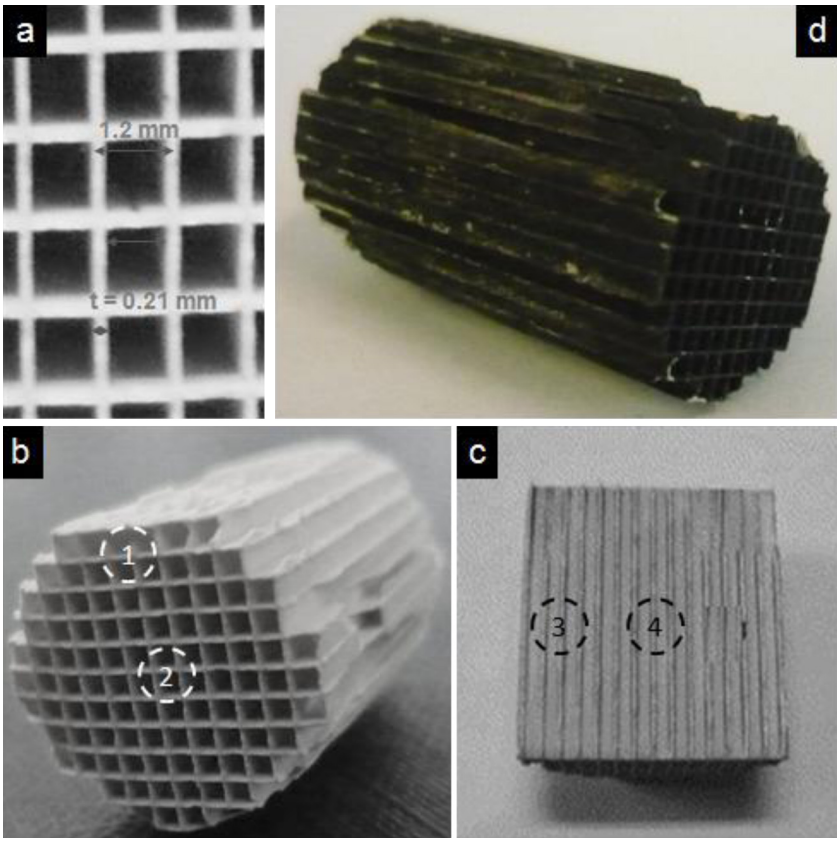

Fig. 1. Geometric characteristics of the honeycomb cordierite (a), scheme of the four zones selected for the SEM–EDS analysis (b and c), and image of one monolithic catalyst prepared in this study (d).

same conditions and the product obtained was referred to as Co/La-CeO_2–S. The calcination step allows the PVOH removal.

2.3. Catalysts characterization

The metal content in the catalysts was determined by inductively coupled plasma atomic emission spectroscopy (ICP-AES) using a Thermo Elemental Iris Intrepid instrument.

X-ray powder diffraction studies (XRD) were carried out on a Bruker instrument, model D8 Advance 500. The diffractograms were recorded using Cu Kα radiation and a graphite monochromator. The scanning ranged from 2° up to 130°, with a step size of 0.03° and 45 s step time. Both powders and monoliths samples were crushed and sieved for these measurements.

The textural characterization was performed by means of nitrogen physisorption at −196 °C using a Micromeritics ASAP2020 instrument. The samples were degassed at 200 °C for 2 h prior to the analysis. In the particular case of the monoliths a sample holder specially built to contain the entire monolith specimen was used. The surface area (S_{BET}) was determined by BET (Brunauer–Emmett–Teller) method. Total pore volume (V_p) was determined from the amount adsorbed at a relative pressure of around 0.99. The pore size distribution and average pore diameter (D_p) were determined by BJH (Barrett–Joyner–Halenda) method from the desorption branch of the isotherm.

The morphology and semi quantitative compositional analyses of the surface were carried out using scanning electron microscopy (SEM, FEI and Hitachi S-2700) with both secondary and backscatter electrons detector. The elemental composition was determined using the energy dispersive X-ray spectroscopy (EDS) with a QUANTA-200. For this purpose the monoliths were sectioned with scalpel to allow measurements of different zones (Fig. 1b and c).

In the particular case of the monolithic catalysts, the adherence of the washcoat to the cordierite honeycomb was evaluated in terms of weight loss after ultrasonic treatment according to the procedure proposed by Yasaki et al. [26]. The calcined coated monoliths were immersed in petroleum ether in a sealed beaker and sonicated for 30 min. Samples were removed, dried and calcined. The weight loss was determined by the difference in the mass of the samples before and after the ultrasonic test. The results are presented in terms of percentage of coating retained on the monolith.

2.4. Catalytic performance evaluation

The catalytic activity of the samples was studied by recording the ignition curves of toluene and ethyl acetate in air. Complete oxidation reactions were carried out in a tubular Pyrex fixed-bed reactor (i.d. 8.9 and 17 mm for powders and monoliths, respectively) at atmospheric pressure submitted to a heating ramp (100–400 °C at 2.0 °C min^{-1}). For powdered samples, 250 mg of catalyst diluted with 1.25 g of SiC of the same particle size were used (bed height 1 cm of approx.). The ignition curves were obtained in 500 cm^3 min^{-1} air stream containing 1000 mg C m^{-3}. The space velocity for experiments performed on powdered and MC250 Co/La-CeO_2 samples was 120,000 cm^3 h^{-1} $g_{cat}{}^{-1}$ while for MC125 Co/La-CeO_2 and MC500 Co/La-CeO_2 was 240,000 and 60,000 cm^3 h^{-1} $g_{cat}{}^{-1}$ respectively (same weight hourly space velocity). Conversion was obtained by CO_2 monitoring by an online IR detector (Vaisala GMT220) and the VOCs disappearance and the production of water by Mass Spectroscopy (Balzers Omnistar) was measured only for ethyl acetate oxidation because previous studies have shown that there are no intermediate products in the catalytic removal of toluene [27,28]. The CO_2 conversion was calculated as the ratio between the CO_2 signal divided by its value

Table 1
Elemental composition (wt%) of the catalysts estimated by ICP analysis.

Sample	Ce	La	Co	Al
Co/La-CeO_2	56.87	5.50	13.94	–
Co/La-CeO_2-S	44.39	4.44	11.41	7.40
MC250 Co/La-CeO_2	3.62 (45.80)[a]	0.32 (4.00)[a]	0.87 (11.00)[a]	34.23

[a] Data into brackets correspond to percentage of the coating.

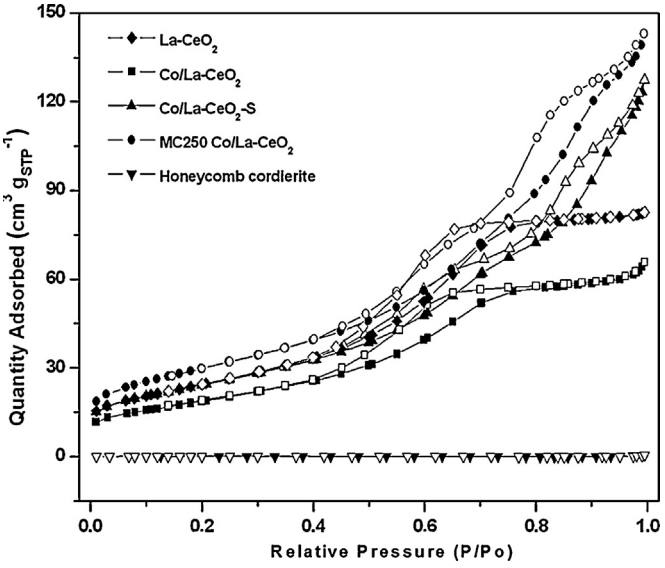

Fig. 2. N_2 physisorption isotherms obtained for the samples of this study. The full and empty symbols correspond to adsorption and desorption branches respectively.

measured when complete conversion at high temperature has been reached. No partial oxidation products neither coke deposition were detected during oxidation of ethyl acetate and toluene. A study of the stability for the powdered and structured catalysts under isothermal reaction conditions was performed during 80 h at high conversion (around 60–80%).

3. Results and discussions

3.1. Powdered catalyst characterization

Table 1 summarizes the compositional results estimated by means of ICP analysis. It should be noticed that the Co content in Co/La-CeO_2 does not significantly differ from the nominal value being this estimated at 15%.

Figs. 2 and 3 show the N_2 adsorption–desorption isotherms obtained and the pore size distribution curves derived from their processing respectively. Table 2 summarizes the main parameters

Table 2
Textural properties of the samples measured by N_2 physisorption at −196 °C.

Sample	S_{BET}[a] ($m^2\ g^{-1}$)	V_p[b] ($cm^3\ g^{-1}$)	D_p[c] (nm)
La-CeO_2	91.1	0.116	3.8
Co/CeO_2	74.2	0.105	4.5
Co/La-CeO_2	68.7	0.097	4.4
Co/La-CeO_2-S	87.8	0.186	6.9
AL20 NYACOL[+]	173.2	0.295	4.8
Cordierite honeycomb	<1	–	–
MC250 Co/La-CeO_2[*]	99.9	0.209	6.5

[+] Analysis carried out for colloidal alumina dried and calcined.
[*] Data expressed per gram of washcoat.
[a] Calculated by BET method.
[b] Determined from the amount adsorbed at $P/P_0 = 0.99$.
[c] Determined by BJH method of the desorption branch.

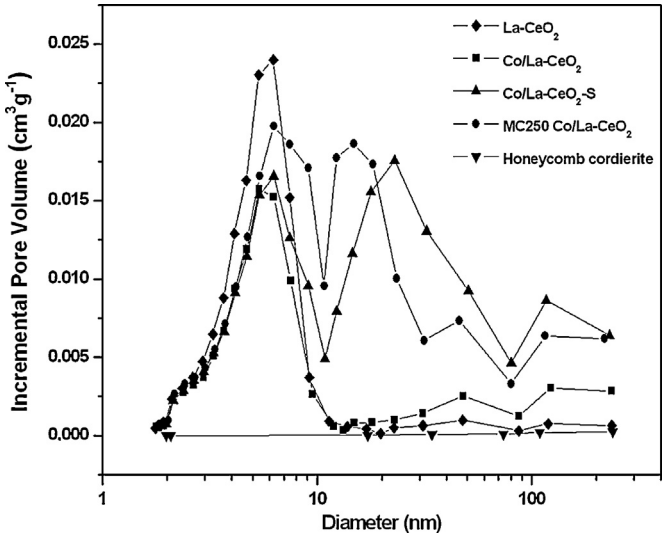

Fig. 3. Pore size distribution obtained from the N_2 physisorption experiments of the samples of this study.

derived from the analysis of these curves and also the results for the La-CeO_2 and Co/CeO_2 are shown. The results indicate that the Co/La-CeO_2 sample exhibits a type IV isotherm that typically is associated to a mesoporous solid, in this case with an average pore size centered around 5 nm (Fig. 3). The slightly higher value of the mean pore diameter in comparison with the support (Table 2) suggests that the small pores are being blocked with the cobalt or eliminated by the calcination step. On the other hand, BET specific surface area of the catalyst decreases with respect to the support as a consequence of the aforementioned disappearance of the narrow pores. Also remarkable, comparison between data obtained for Co/CeO_2 and Co/La-CeO_2 suggests that modification of ceria by lanthanum does not induce significant changes of the textural properties.

X-ray diffraction was used to determine the nature of the phases present in the samples (Fig. 4). It should be noticed that for the Co/La-CeO_2 catalyst and the La-CeO_2 support, peaks are detected corresponding to the typical face–centered cubic (fcc) fluorite structure of CeO_2 (JCPDS 03-065-5923). However, a detailed analysis of these peaks reveals a slight shift of their position toward lower 2θ values respect that characteristic of pure ceria, for example from

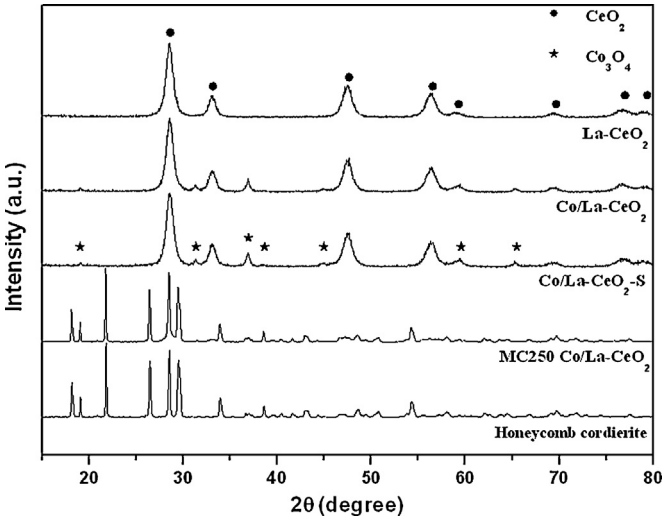

Fig. 4. XRD diffractograms obtained for the samples of this study.

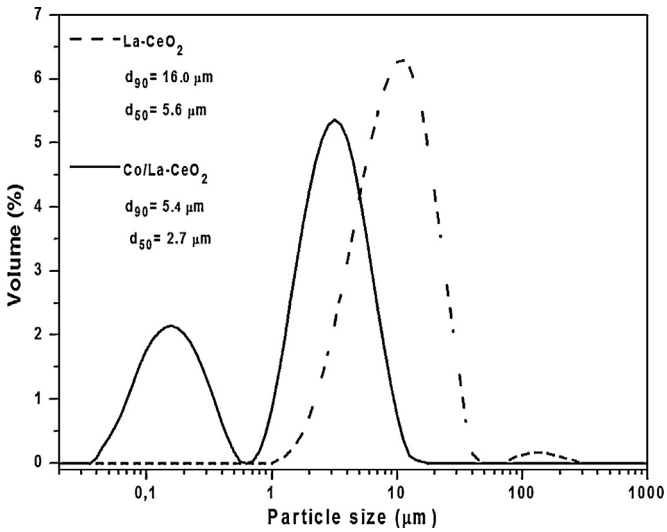

Fig. 5. Particle size distribution estimated by means of granulometry.

28.555 to 28.50 for the (1 1 1) planes. This finding is in good agreement with the modification of the lattice parameters of ceria by the lanthanum incorporation [11]. The diffractogram also clearly exhibit crystalline features of Co_3O_4 spinel (JCPDS 01-076-1802) of the Co/La-CeO_2.

3.2. Washcoating of the monoliths

The objective was to prepare a slurry from the previously synthesized powdered catalyst allowing further forming of a homogeneous layer, strongly adhered onto the monolith walls. To reach these objectives, a proper adjustment of several parameters such as the solids content including additives, granulometry, viscosity and pH is needed. Fig. 5 shows the particle size distribution measured for both the La-CeO_2 support and the Co/La-CeO_2 catalyst. The results obtained indicate that the incorporation of the cobalt phase onto the support allows some disaggregation of the material showing a significant fraction of particles with lower size appearing. Also noticeable, in the case of the cobalt catalyst a value of 5.0 μm has been estimated for the d_{90} parameter. According to Agrafiotis et al. [29] this value is low enough to allow the direct use of the material for washcoating purposes without further grinding.

Another parameter that must be properly controlled is the zeta potential of the powdered catalyst as it allows establishing the pH range in which the slurry of this powder will be stable as far as the particles do not tend to agglomerate [23]. Fig. 6 shows the result of these measurements, indicating an isoelectrical point of 6.4. As can be noticed at pH 4 the value of zeta potential is around 30 mV that is considered by Vallar et al. [30] as a high value ensuring the repulsion between particles and good slurry stability. Additionally, from a chemical point of view the Co_3O_4 phase should be thermodynamically stable against dissolution at pH 4 [31]. Consequently, the suspensions were prepared adjusting the pH to a value of 4 with acetic acid. Preliminary tests were carried out to determine the solids content of the slurry, using as additives colloidal alumina as binder and alcohol polyvinyl as dispersant. Twenty-five wt% solids content was the optimum value, showing a slurry viscosity of 18.3 mPa s, this value being in the range recommended by several authors as [32–34].

In order to evaluate the efficiency of the dip-coating procedure, it was carried out in consecutive steps to measure the amount of washcoating loading deposited at each step for different pieces of monoliths until getting the target load (125, 250 and 500 mg of catalyst). The results for the latter are shown in Fig. 7. The loading

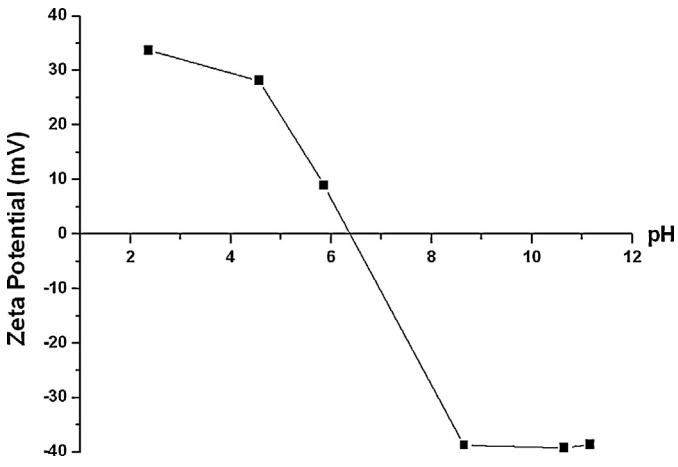

Fig. 6. Zeta potential vs pH for the Co/La-CeO_2 catalyst.

obtained is a linear function of the number of coating steps, but the slope decreases after the third coating. This latter effect could be due to no proper water elimination during the dried step between each dip-coating. It should be taken into account that the amount retained is determined by the surface roughness, the slurry viscosity and the surface tension [35], despite those difficulties our results displaying an excellent reproducibility. Fig. 1d shows an image of one of the washcoated monoliths prepared in this work.

3.3. Monoliths characterization

The metal content of the monoliths was determined by ICP-AES, the results are shown in Table 1. Considering the use of additives in the preparation of the slurry, the cobalt amount in the calcined slurry accordingly decreases in comparison with Co/La-CeO_2. If data corresponding to MC250 Co/La-CeO_2 are referred to gram of washcoat the elemental content of La, Ce and Co for the monolithic catalyst is in good agreement with that found for the powdered catalyst. In the particular case of Al the higher content in the former should be related to the presence of this element in the cordierite.

Table 2 summarizes the textural properties for the bare cordierite, the calcined slurry and the coated monolith. The specific surface area, pore volume and pore diameter of the monolithic

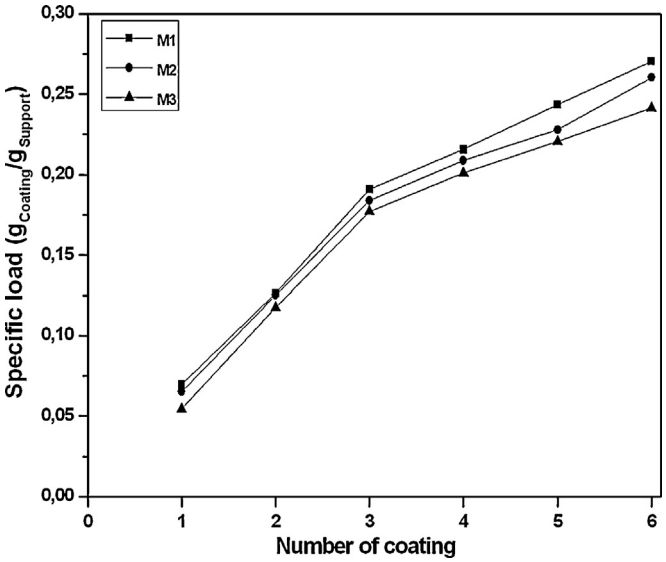

Fig. 7. Cumulative specific load vs number of coating steps obtained on different honeycomb cordierite pieces (M1, M2, M3) coated with a stable Co/La-CeO_2 slurry.

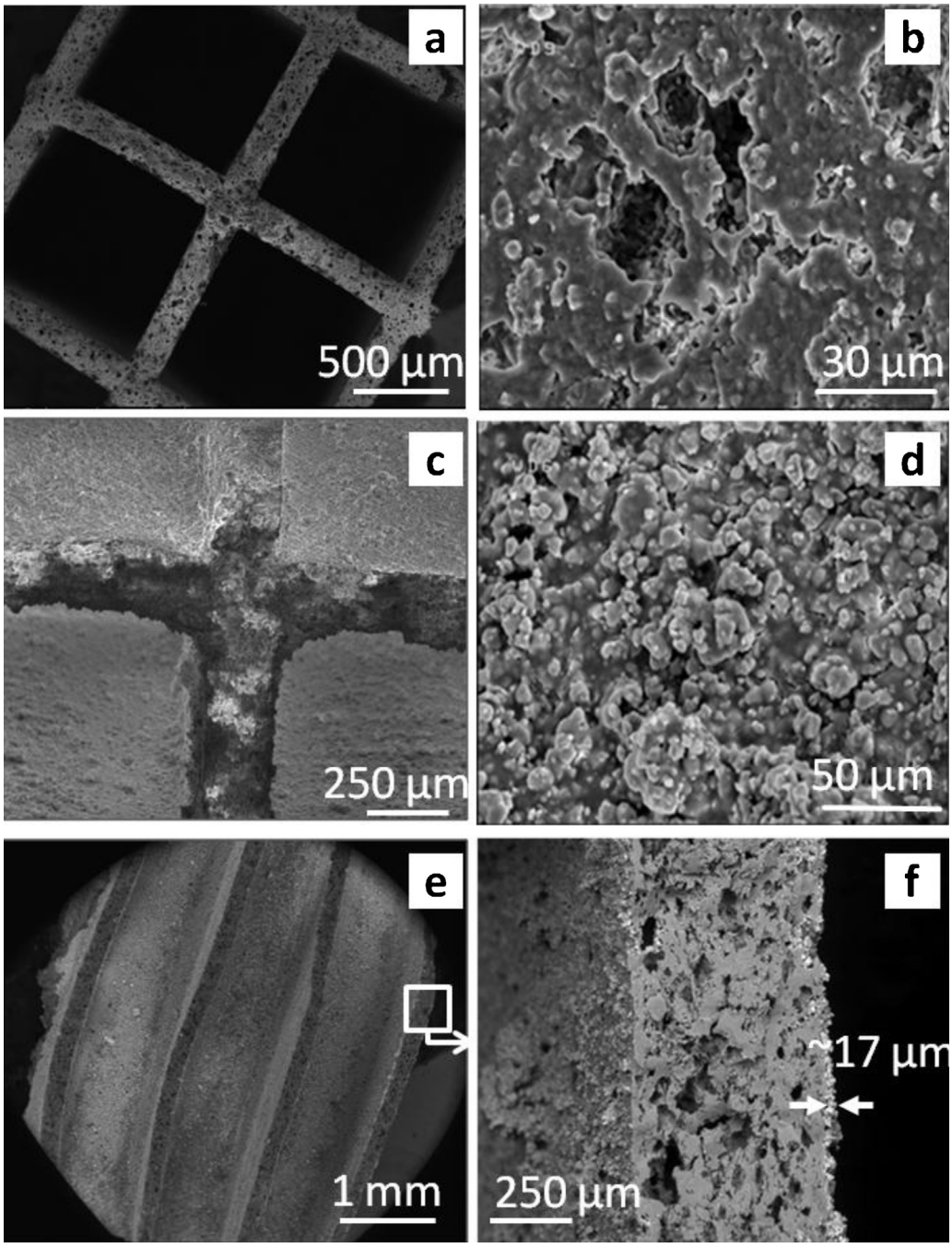

Fig. 8. SEM images of the bare honeycomb cordierite (a and b) and the MC250 Co/La-CeO_2 monolithic catalyst (c–f). A magnification of the indicated area of (e) image showing the thickness of the washcoat layer is included in the (f) image.

catalyst increased compared to the powdered catalyst. Other changes with respect to Co/La-CeO_2 can be seen in Figs. 2 and 3. The isotherms (Fig. 2) of the slurry calcined and the monolithic catalyst present a new adsorption step at p/p_0 0.8–0.9 corresponding to the presence of new mesopores wider than 10 nm reported on Fig. 3. These changes must be related to the presence of the colloidal alumina used as additive for the slurry preparation, since the porous content in the cordierite is negligible as reported in Table 2. This alumina acts as a binder favoring the aggregation to the powder and forming new mesopores between these particles.

The XRD diffractograms (Fig. 4) reveal that both cerium and cobalt phases can be also observed in the pattern of Co/La-CeO_2–S while the one for MC250 Co/La-CeO_2 resembles that of pure cordierite due to the composition of this sample which is dominated by the substrate phase. In this case is very difficult to detect the Co and Ce phases, although Rietveld analysis (results not shown) suggests that they are present as spinel and ceria respectively.

The surface topography of the monolithic catalysts has been studied by SEM (Fig. 8). The images obtained for all the four zones studied on the coated cordierite were very similar, so only images of zone 1 are presented. The comparison between the surface of the bare cordierite (Fig. 8b) and that of MC250 Co/La-CeO_2 sample (Fig. 8d) reveals the appearance of particles agglomerates in the latter, which are irregular in shape and size. Also evident, the macroporosity of the support disappears as consequence of the

Table 3
Elemental composition (excluding Al) estimated by SEM–EDS analysis and surface covered (%) estimated from EDS-mapping in the four different zones selected in the washcoated monolith (shown in Fig. 1).

Zone	Co (wt%)	Ce (wt%)	La (wt%)	Covering by Co (area %)	Covering by Ce (area %)
1	15	80	5	26	44
2	15	77	8	35	66
3	15	78	7	25	47
4	14	77	8	23	54

coating. This result suggests the uniform distribution of the catalyst over the cordierite.

The thickness of the washcoating layer for the monolith loaded with 250 mg of catalyst ranges between 15 and 20 μm (Fig. 8f). For the rest of the monoliths it can be assumed proportionality between the load and the thickness. This simple measurement can be done by means of backscattered electron (BSE) SEM images. Since heavy elements in the washcoat (Ce, La and Co; higher atomic number) backscatter electrons more strongly than the much lower atomic number elements from the cordierite monolith (Mg, Al and Si) the areas containing the heavier elements appear brighter in the image. Hence, the dark bands in Fig. 8e and f correspond to the cordierite walls, whereas the brighter regions in between the dark bands image the washcoat [36].

It must be also noticed that according to Fig. 8a and c, the coating does not tend to accumulate at the corners of the cordierite wall, at least in a significant amount. The observations so far commented suggest that the interaction between the coating layer and the cordierite may be very strong. This is also supported by the results of the adherence test, which indicated that 98% of the washcoating remained attached to the cordierite after the ultrasound treatment.

Finally, the homogeneity of the chemical composition of the washcoat has been analyzed by means of SEM–EDS (Table 3). First, it is worth noting that no matter the analyzed zone of the monolith the relative elemental composition of the washcoat does not change significantly. This is indicative of a good interaction between the different components of the catalytic phase. Moreover, the cobalt content estimated by this technique is in reasonable agreement with that obtained by ICP analysis of the powdered and monolithic catalyst (Table 1). The compositional maps for the different elements built from the EDS data corresponding to areas of 800 μm × 800 μm (results not shown) also indicate an uniform distribution of Co and Ce. The percentage of surface covered by each element was additionally calculated (Table 3), demonstrating again a homogeneous scenario.

3.4. Catalytic activity

Activity tests of toluene and ethyl acetate oxidation were performed to evaluate the potential of the Co/La-CeO_2 catalyst formulation here proposed. For this purpose comparison with a noble metal deposited on the same support has been made (Pt/La-CeO_2 sample). In this case platinum has been chosen considering its well-known performance in these reactions according to literature [28,37]. The La-CeO_2 support along with the Co/CeO_2 catalyst have been also studied as references. The ignition curves corresponding to the conversion percentage was calculated from CO_2 signal (total mineralization) while the furnace is cooled down with a programmed ramp after a preliminary reaction period at 400 °C. This starting protocol has been carried out following the suggestions proposed by Paulis et al. [27] since the ignition curves obtained for Pt/La-CeO_2 and Co/La-CeO_2 increasing the temperature presented CO_2 peaks that produced conversions percentages calculations higher than 100% (results not shown). It has been reported that

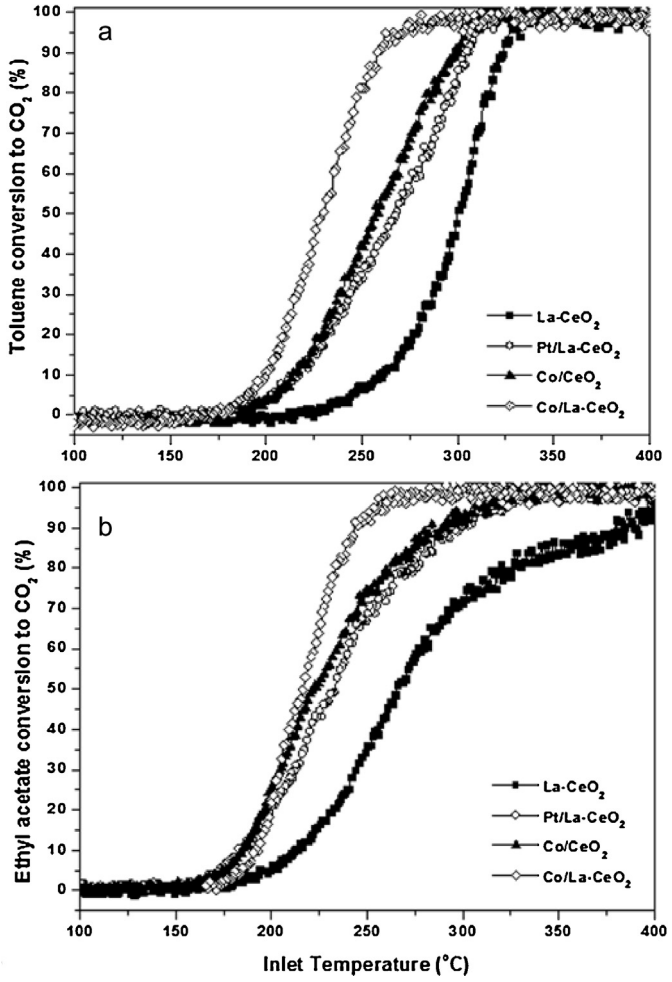

Fig. 9. Ignition curves for toluene (a) and ethyl acetate (b) oxidation over the powdered catalysts.

when the activity of the active phase is high enough to start the oxidation at a sufficiently low temperature, close to that at which the adsorption and desorption of the different species take place, all these processes will be coupled giving rise to the above-cited CO_2 peaks [27].

Fig. 9 and Table 4 show the main derived results respectively that correspond to the VOCs oxidation over the whole set of samples. During the catalytic combustion of toluene and ethyl acetate, the only products detected were CO_2 and H_2O, indicating that complete combustion occurs in both reactions. In Fig. 9 it can be observed that the addition of cobalt on the La-CeO_2 support notably improves its activity in both reactions. In this way, for Co/La-CeO_2 the conversion of toluene starts at about 180–200 °C and it is completed below ca. 260 °C while for platinum catalyst the toluene conversion

Table 4
Temperatures for 10%, 50% and 90% of conversion in the catalytic oxidation of toluene and ethyl acetate over the samples investigated.

Sample	Toluene			Ethyl acetate		
	T_{10} (°C)	T_{50} (°C)	T_{90} (°C)	T_{10} (°C)	T_{50} (°C)	T_{90} (°C)
La-CeO_2	259	300	323	213	266	386
Co/CeO_2	214	257	298	185	222	290
Pt/La-CeO_2	215	267	305	184	232	297
Co/La-CeO_2	199	229	258	193	217	244
MC125 Co/La-CeO_2	234	259	295	224	247	274
MC250 Co/La-CeO_2	226	253	286	208	242	282
MC500 Co/La-CeO_2	221	249	286	197	242	282

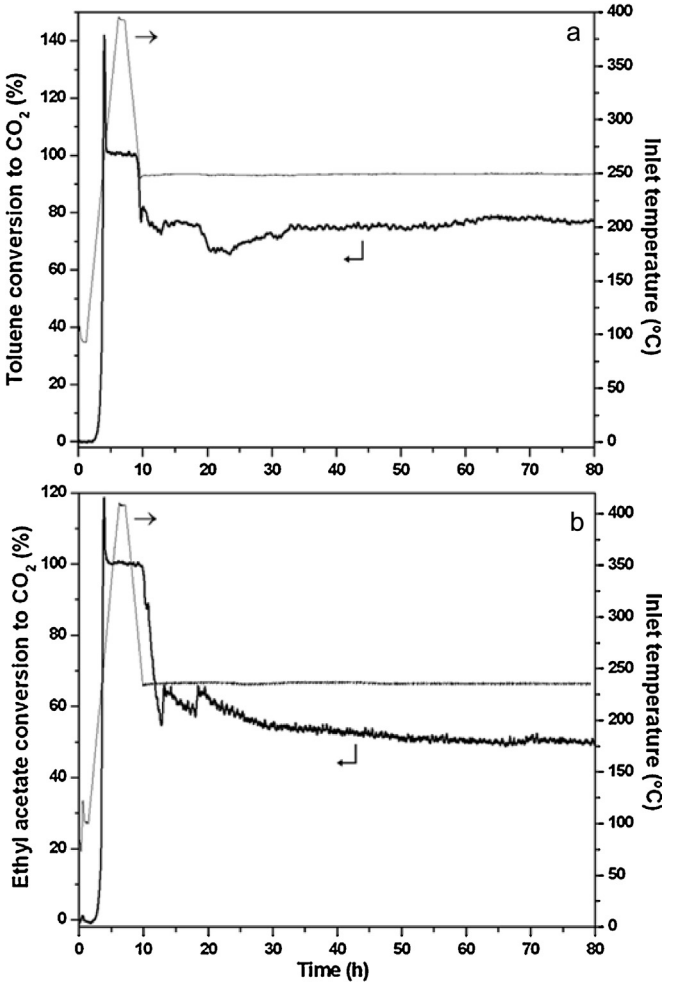

Fig. 10. Stability test for toluene (a) and ethyl acetate (b) oxidation over Co/La-CeO_2 catalyst.

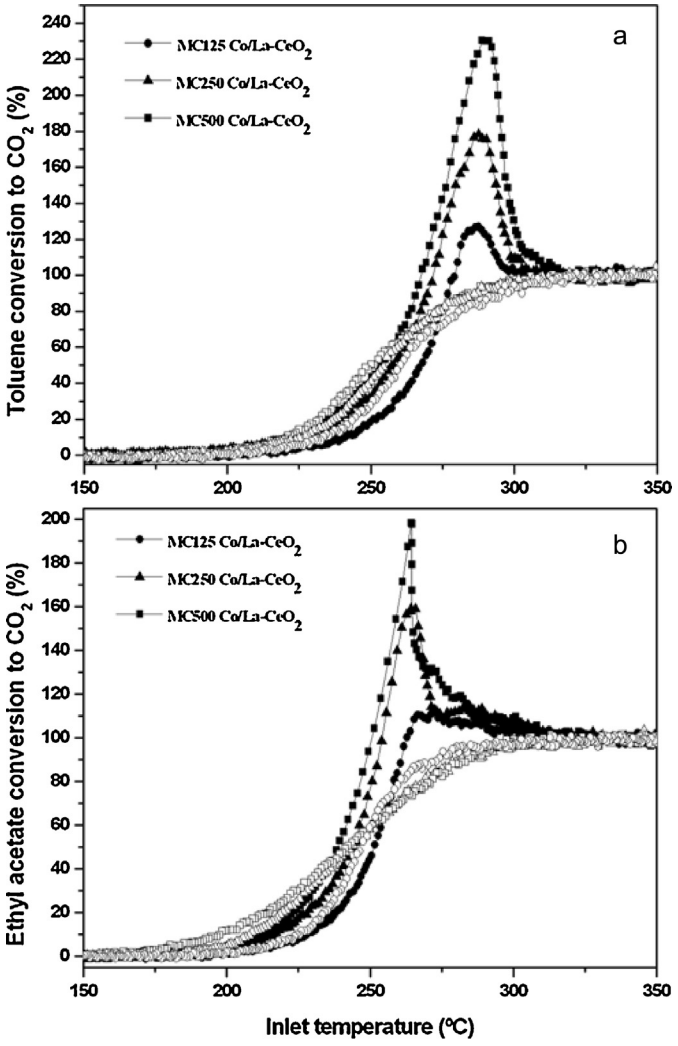

Fig. 11. Ignition curves for toluene (a) and ethyl acetate (b) oxidation over the monolithic catalysts with different washcoating loading. The filled and empty symbols represent the rising and lowering curves respectively.

starts at similar temperatures but it is completed at ca. 310 °C (Fig. 9a). On the other hand, for cobalt catalyst the ethyl acetate conversion begins at around 160–180 °C and it completed below ca. 270 °C whereas for the platinum catalyst the ethyl acetate conversion begins at lower temperatures however it is completed at ca. 325 °C (Fig. 9b). It is remarkable that cobalt catalyst presents higher activity even than platinum catalyst under the experimental conditions used in this study. Likewise, Co/La-CeO_2 presents better activity over the ethyl acetate oxidation than Pt/Al_2O_3 catalyst studied in [3] exhibiting a T_{50} around 280 °C and similar value of T_{50} in comparison with catalytic oxidation of toluene over a Pt/Al_2O_3 catalyst (T_{50} = 210 °C) [21]. Moreover, comparing with some results reported in the literature it can be confirmed the good activity of our catalyst. Liotta et al. [38] evaluated the oxidation of toluene over Co_3O_4–CeO_2 mixed oxide catalysts with different cobalt loadings obtaining a T_{50} = 233 °C for a Co_3O_4(30%)–CeO_2 sample which presents the best behavior, this value being very close to the one here obtained with Co/La-CeO_2 but with a lower cobalt loading, while T_{50} for the Co_3O_4(15%)–CeO_2 sample was 328 °C, 100 °C higher than for our catalyst. Alifanti et al. [15] found a T_{50} = 244 °C for the toluene oxidation over a bulk $LaCoO_3$ perovskite catalyst, about 15 °C higher than Co/La-CeO_2. Other results are very similar, such as those reported in [4] by Todorova et al. who obtained a T_{50} around 220 °C for the ethyl acetate oxidation run over a Mn–Co mixed oxide catalyst. These results indicate that combination of cobalt, lanthanum and ceria can be attractive not only if they form a mixed oxide [38] but also upon the metal deposition onto a lanthanum-modified ceria support as it is proposed in this work.

Also significant, comparison between Co/La-CeO_2 and Co/CeO_2 in Fig. 9 and Table 4 demonstrates that the modification of the ceria support with lanthanum has a beneficial effect in both reactions. This might be related to the improvement of ceria reducibility by lanthanum inclusion, in agreement with other authors who emphasize the role of the redox properties in the mechanism of VOCs oxidation reactions [18,38].

The catalytic stability of Co/La-CeO_2 for toluene and ethyl acetate oxidation was also investigated. The catalytic performance was evaluated at a reaction temperature of 250 °C for toluene oxidation and of 236 °C for ethyl acetate oxidation for 80 h beginning with the activation of catalyst at 400 °C. The temperatures leading to ca. 80% and ca. 60% conversion for toluene and ethyl acetate respectively were selected to detect the possible catalyst deactivation. Flow gas, heating rate and pressure conditions were the same described before in Section 2.4. Fig. 10 shows the results of this study. It can be observed that, despite at first hours the conversion percentage is very sensible to slight perturbations of the temperatures, once the signal has been stabilized, no catalyst deactivation takes place under the conditions evaluated for toluene and a slight activity lose that tends to stabilize is observed in the ethyl acetate oxidation.

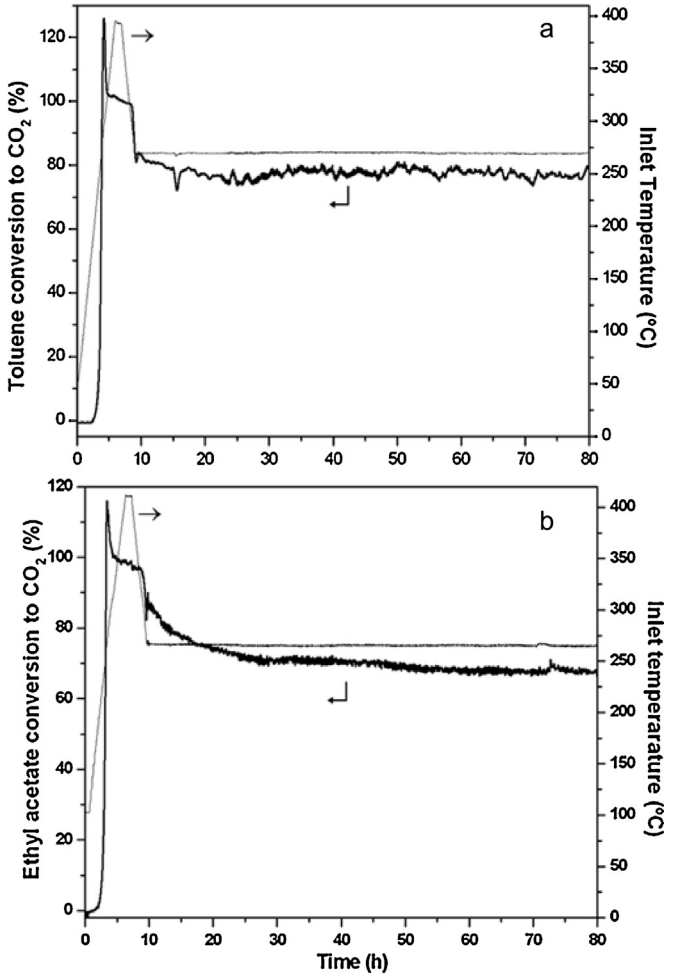

Fig. 12. Stability test for toluene (a) and ethyl acetate (b) oxidation over MC250 Co/La-CeO_2 monolithic catalyst.

Once the cordierite monoliths were washcoated with the 25 wt% slurry, their catalytic behavior was also evaluated in the oxidation of toluene and ethyl acetate. The results are shown in Fig. 11 and Table 4. It can be appreciated over-conversion peaks only in the heating up branch produced by the coupling between the adsorption–desorption phenomena and the catalytic oxidation that was previously reported by Paulis et al. [27]. As the height of the peak depends on the amount of reactants and products adsorbed, the peak increases as the amount of catalyst loaded on the monolith increases. For the oxidation of toluene, in general, the washcoating loading does not seem to have a significant effect on the catalytic activity except for the difference presented for MC125 Co/La-CeO_2 of almost 10 °C for the 90% of conversion (Table 4). While for the oxidation of ethyl acetate the monolithic catalysts with 250 and 500 mg of catalyst present higher activity than MC125 Co/La-CeO_2 (Table 4). Those differences are evident in the T_{50} and T_{90} that deviate each other between 5 and 10 °C respectively. If the increase of catalyst load does not produces increase in activity, this shows that there is not kinetic control of the reaction suggesting external diffusional limitations that are frequent in monoliths for combustion processes [39].

The comparison between the catalytic data corresponding to the powdered Co/La-CeO_2 catalyst and the MC250 Co/La-CeO_2 sample with similar catalyst loading (Table 4) reveals a slight increase in the T_{10}, T_{50} and T_{90} temperatures. Nevertheless, this might be reasonably related to the differences in the contact mode between the catalyst and the gas phase. In the case of fixed beds with small catalyst particles, both interparticle and intraparticle diffusional limitations are minimized with very turbulent flow, but at the cost of high pressure drop. In the case of honeycomb monoliths, the flow inside the channels is deeply laminar, but the pressure drop is negligible, which is a prerequisite for many environmental processes. In order to compare with some results reported in the literature, e.g., Zhou et al. [40] prepared a metal transition-containing catalyst washcoated onto a ceramic monolith to evaluate the toluene oxidation and the monolithic catalyst that showed the best catalytic activity reached a T_{50} = 260 °C, value close to that achieved in our test results for all the monoliths. Other results were reported by Aguero et al. [41] for both reactions over MnO_x supported on metallic monoliths. These authors found that the T_{50} values for toluene and ethyl acetate oxidation corresponding to the most active sample were 301 and 230 °C, respectively. In this work our monolithic catalysts present lower T_{50} in the toluene oxidation and slightly higher T_{50} in the ethyl acetate oxidation. Therefore, the catalyst formulation proposed keeps being attractive even when supported onto a cordierite monolith.

As for the powdered catalyst, a catalytic stability study was performed for MC250 Co/La-CeO_2 at the same conditions, except temperatures reaction. The toluene oxidation was evaluated at 268 °C, temperature corresponding to ca. 80% of conversion, and the ethyl acetate oxidation was carried out at 266 °C, temperature equivalent to 70% of conversion. Fig. 12 shows the results. It can be noticed, as for the powdered catalyst, no significant evidence of deactivation for the monolithic catalyst for toluene and a longer stabilization time for ethyl acetate before reaching the steady state.

4. Conclusions

In this work a novel Co/La-CeO_2 catalyst formulation with 15 wt.% cobalt content has been prepared by a simple impregnation method, characterized and tested for catalytic VOCs oxidation. Its light-off temperature was around 40 °C below that of a Pt reference catalyst under the same experimental conditions. Considering the advantages of the monolithic design with regard to powder for environmental process, a catalyst slurry with appropriate properties was prepared and successfully used for washcoating cordierite honeycombs. Physico-chemical characterization showed that the compositional and structural properties of the powdered catalyst were preserved upon being supported on the cordierite monolith while the textural properties were improved due to the inclusion of colloidal alumina in the slurry formulation. The study of the calcined slurry as an intermediate step of the washcoating method reinforced this conclusion. In the particular case of the cobalt, a Co_3O_4 spinel phase was confirmed by XRD. Also significant, the washcoating evidenced high adherence (98% catalyst retained), SEM images showed uniform distribution of the catalyst layer with thickness between 15 and 20 μm and EDS analyses suggested that catalyst was deposited in a homogeneous way. The powdered catalyst and monoliths prepared by washcoating method had not only a good activity, but in the same order or even better than that reported in the literature in the oxidation of toluene and ethyl acetate in other similar formulations but also a remarkable catalytic stability for both reactions.

Acknowledgements

The authors thank the financial support by the Ministry of Science and Innovation of Spain/FEDER Program of the EU (Project MAT2008-00889/NAN and CSD2009-00013), the Junta de Andalucía (Groups FQM-110 and FQM-334) and UPV/EHU (GIU 11/13). We also acknowledge the Cadiz University SCCyT for using

its facilities and to Dr. Mª Jesús Lázaro from the Institute of Carbochemistry of Zaragoza (CSIC) in Spain who provided us the cordierite block.

References

[1] J.N. Armor, Applied Catalysis B: Environmental 1 (1992) 221–256.
[2] G. Busca, M. Daturi, E. Finocchio, V. Lorenzelli, G. Ramis, R. Willey, Catalysis Today 33 (1997) 239–249.
[3] P. Papaefthimiou, T. Ioannides, X.E. Verykios, Applied Catalysis B: Environmental 13 (1997) 175–184.
[4] S. Todorova, A. Naydenov, H. Kolev, K. Tenchev, G. Ivanov, G. Kadinov, Journal of Materials Science 46 (2011) 7152–7159.
[5] S. Todorova, H. Kolev, J.P. Holgado, G. Kadinov, C. Bonev, R. Pereniguez, A. Caballero, Applied Catalysis B: Environmental 94 (2010) 46–54.
[6] T.S.C. Law, C. Chao, G.Y.W. Chan, A.K.Y. Law, Atmospheric Environment 37 (2003) 5433–5437.
[7] J. Lamonier, A. Boutoundou, C. Gennequin, M.J. Perez-Zurita, S. Siffert, A. Aboukais, Catalysis Letter 118 (2007) 165–172.
[8] T. Miki, T. Ogawa, M. Haneda, N. Kakuta, A. Ueno, S. Tateishi, S. Matsuura, M. Sato, Journal of Physical Chemistry 94 (1990) 6464–6467.
[9] A. Bueno-López, K. Krishna, M. Makkee, J.A. Moulijn, Journal of Catalysis 230 (2005) 237–248.
[10] S. Bernal, G. Blanco, G. Cifredo, J.A. Perez-Omil, J.M. Pintado, J.M. Rodriguez-Izquierdo, Journal of Alloys and Compounds 250 (1997) 449–454.
[11] S. Bernal, G. Blanco, A. El Amarti, G. Cifredo, L. Fitian, A. Galtayries, J. Martin, J.M. Pintado, Surface and Interface Analysis 38 (2006) 229–233.
[12] F. Wyrwalski, J. Giraudon, J. Lamonier, Catalysis Letter 137 (2010) 141–149.
[13] L.F. Liotta, G. di Carlo, G. Pantaleo, A.M. Venezia, G. Deganello, Applied Catalysis B: Environmental 66 (2006) 217–227.
[14] L.F. Liotta, G. di Carlo, G. Pantaleo, G. Deganello, Applied Catalysis B: Environmental 70 (2007) 314–322.
[15] M. Alifanti, M. Florea, V.I. Parvulescu, Applied Catalysis B: Environmental 70 (2007) 400–405.
[16] J. Kirchnerova, M. Alifanti, B. Delmon, Applied Catalysis A: General 231 (2002) 65–80.
[17] A.F. Lucredio, G. Jerkiewicz, E.M. Assaf, Applied Catalysis B: Environmental 84 (2008) 106–111.
[18] J. Luo, M. Meng, Y. Qian, Z. Zou, Y. Xie, T. Hu, T. Liu, J. Zhang, Catalysis Letter 116 (2007) 50–56.
[19] Z. Zou, M. Meng, Y. Zha, Y. Liu, Journal of Materials Science 43 (2008) 1958–1965.
[20] A. Cybulski, J.A. Moulijn, Catalysis Reviews – Science and Engineering 36 (1994) 179–270.
[21] S. Ojala, S. Pitkaaho, T. Laitinen, N.N. Koivikko, R. Brahmi, J. Gaalova, L. Matejova, A. Kucherov, S. Paivarinta, C. Hirschmann, T. Nevanpera, M. Riihimaki, M. Pirila, R.L. Keiski, Topics in Catalysis 54 (2011) 1224–1256.
[22] P. Avila, M. Montes, E.E. Miro, Chemical Engineering Journal 109 (2005) 11–36.
[23] V. Tomasic, F. Jovic, Applied Catalysis A: General 311 (2006) 112–121.
[24] J.L. Williams, Catalysis Today 69 (2001) 3–9.
[25] J.J. Spivey, Industrial & Engineering Chemistry Research 26 (1987) 2165–2180.
[26] S. Yasaki, Y. Yoshino, K. Ihara, K. Ohkubo, US Patent 5208206 (1993).
[27] M. Paulis, L.M. Gandia, A. Gil, J. Sambeth, J.A. Odriozola, M. Montes, Applied Catalysis B: Environmental 26 (2000) 37–46.
[28] N. Burgos, M. Paulis, M.M. Antxustegi, M. Montes, Applied Catalysis B: Environmental 38 (2002) 251–258.
[29] C. Agrafiotis, A. Tsetsekou, Journal of the European Ceramic Society 20 (2000) 815–824.
[30] S. Vallar, D. Houivet, J. El Fallah, D. Kervadec, J.M. Haussonne, Journal of the European Ceramic Society 19 (1999) 1017–1021.
[31] F.M. Doyle, R. Woods, G. Kelsall (Eds.), Electrochemistry in Mineral and Metal Processing 8 (EMMP 8), 6th ed., The Electrochemical Society, New Jersey, USA, 2010.
[32] C. Agrafiotis, A. Tsetsekou, Journal of Materials Science 35 (2000) 951–960.
[33] T. Tao, J. Torns, B. Usiak, US Patent 6903051B2 (2005).
[34] A. Eleta, P. Navarro, L. Costa, M. Montes, Microporous and Mesoporous Materials 123 (2009) 113–122.
[35] D.M. Frías, S. Nousir, I. Barrio, M. Montes, L.M. Martínez T, M.A. Centeno, J.A. Odriozola, Applied Catalysis A: General 325 (2007) 205–212.
[36] J.C. Hernández-Garrido, D.M. Gómez, D. Gaona, H. Vidal, J.M. Gatica, O. Sanz, J.M. Rebled, F. Peiró, J.J. Calvino, Journal of Physical Chemistry C 117 (2013) 13028–13036.
[37] P. Papaefthimiou, T. Ioannides, X.E. Verykios, Catalysis Today 54 (1999) 81–92.
[38] L.F. Liotta, M. Ousmane, G. di Carlo, G. Pantaleo, G. Deganello, A. Boreave, A. Giroir-Fendler, Catalysis Letter 127 (2009) 270–276.
[39] S.Y. Joshi, M.P. Harold, V. Balakotaiah, Chemical Engineering Science 65 (2010) 1729–1747.
[40] J. Zhou, D. Wu, W. Jiang, Y. Li, Chemical Engineering & Technology 32 (2009) 1520–1526.
[41] F.N. Aguero, B.P. Barbero, L. Costa Almeida, M. Montes, L.E. Cadus, Chemical Engineering Journal 166 (2011) 218–223.